IN-SITU DEPOSTION OF PRESSURE AND TEMPERATURE SENSITIVE E-SKIN FOR ROBOTIC APPLICATIONS

Jarred W. Fastier-Wooller[1]*, Trung Hieu Vu*[1]*, Canh-Dung Tran*[2]*, Toan Dinh*[2]*, Van Thanh Dau*[1,3]*, and Dzung Viet Dao*[1,4]
[1]School of Engineering and Built Environment, Griffith University, Southport, QLD 4222, Australia
[2]School of Mechanical and Electrical Engineering, University of Southern Queensland, QLD 4350, Australia
[3]Centre for Catalysis and Clean Energy - Griffith University
[4]QLD Micro- and Nanotechnology Centre, Griffith University, Brisbane, QLD 4111, Australia

ABSTRACT

The development of a multimodal sensing platform with multiple layers for electronic skin (e-skin) sensing of temperature and pressure has attracted considerable interest to practical applications in soft robotics, human-machine interfaces, and wearable health monitoring. In this work, we demonstrated a new platform technology with multiple sandwiched layers of highly oriented carbon nanotube membrane and polyacrylonitrile for the integration of pressure and temperature sensory functionalities into a single platform that is thin, ultra-lightweight, flexible, and wearable. The key technology of *in situ* deposition of sensor platform on objects or in robot interface makes this a unique method for the development of e-skins for robotic applications, offering a new approach to wearable electronics and portable health care.

KEYWORDS

Electrospinning, e-skin, carbon nanotube, polyacrylonitrile, pressure/temperature sensor.

INTRODUCTION

Demand for smart multifunctional sensing in e-skins has urged the advancements in robotic designs and applications. As robotics become more important in our daily life, designs and applications of robotics have been driven towards multimodal sensing capability, industrious functionality, ergonomic interaction between robotics and humans, and the use of green materials and lifeforms. Electronic-skins (e-skins) and their materials are of considerable interest in the science and engineering community and usually focus on stress/strain and pressure sensing, temperature, humidity and other physical detecting. E-skins have demonstrated as a more advanced, functional, and versatile platform in performing various physical measurements, such as pressure and temperature [1].

Recent works in e-skin technologies have shown a wide range of high performing devices using complex techniques to create micro/nano structured pillars to improve sensitivity [2], [3]. However, little progress has been shown *in situ* fabrication for full integration of sensors into existing devices. E-skin research can be classified as make-and-transfer which has difficulties for sensor integration due to adhesion on curved and non-uniform surfaces. Works have focused on altering designs and material selection to better adhere and integrate sensors [4], [5]. Performing *in situ* fabrication is desired for e-skins because it requires very thin sensing layer that is conformably integrated over different geometry surfaces. This poses improvements to comfort, adhesion, and durability.

In this work, a thin and porous pressure and temperature sensitive e-skin is developed using a multi-layer structure of carbon nanotube (CNT) and polyacrylonitrile (PAN) membranes. Electrospinning is used for *in situ* fabrication of the e-skin with its capability of integration on existing devices. Our sensitive e-skin can be either manufactured and then transferred to existing surfaces or fabricated directly on the rubber end effector of a robot gripper, showing a simple *in situ* fabrication process with a high aptitude for a broad range of robotic applications.

DESIGN AND FABRICATION

Design

In this work, a Baxter research robot with a maximum reported force of 11 N was used to illustrate the present *in situ* fabrication method [6]. The robot finger generates an estimated maximum pressure of up to approx. 80 kPa when contacting with the entire surface of the gripper to hold an object such as a pen at full force. The Baxter robot curved rubber end effectors are used in this work as the pre-existing platform. The rubber end effector is not ideal for make-and-transfer style sensors due to issues adhering the surfaces of the sensor and fingertip without impacting on the sensing performance and physical properties. Attaching a very thin sensor that conformably covers the end effector is desirable to maximise gripping ability of devices. Two ultra-lightweight and highly flexible materials that are able to contour to the surface of the end effector like a layer of skin were chosen as the base of our multi-layered capacitive and resistive device. The chosen materials are CNT and PAN, where CNT is used as a conductor and PAN as a dielectric.

The features of the sandwiched structure and the selected materials allow our device to have two main functions, to sense pressure and temperature, without additional circuitry or complex fabrication procedures. The structure of the present device was designed to measure pressure (capacitance) between the two CNT layers which are separated by a soft and porous layer of PAN. The temperature (resistance) can be measured by the effect of temperature on a layer of CNT, the change of capacitance caused by the variance of permittivity, and any physical deformation of PAN and CNT due to thermal expansion. The outermost CNT layer protected by an ultra-thin and porous PAN layer allows heat to transfer through but protects the dedicated CNT temperature sensor (Figure 1 -

Top figure).

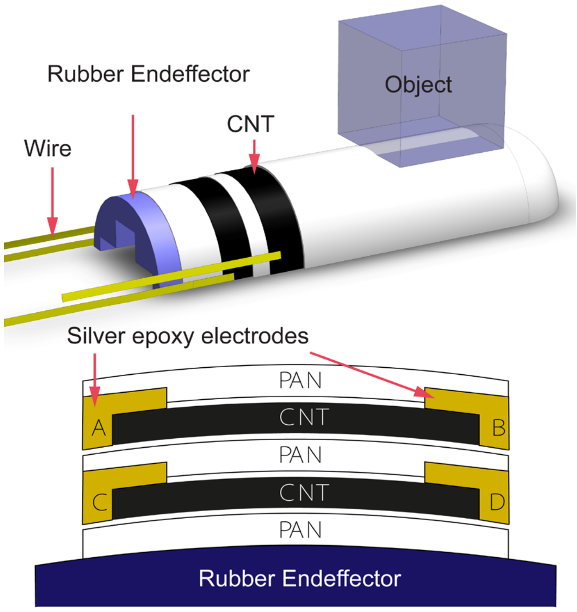

Figure 1. CNT-PAN based sandwiched sensor: (Top) conceptual design of the proposed sensor device and (Bottom) structure of sensing device, electrodes A-B for sensing temperature and electrodes B-C for sensing pressure, electrode D optional.

Sensing Principle

Capacitive pressure sensors

The CNT layers provide a surface area separated by a porous dielectric of PAN nano-fibre to form a capacitor, which serves as a capacitive sensor detecting the deformation by sensing the distance between the two conductive CNT layers on either side of the porous PAN dielectric. The formula for this is well known as,

$$C_o = \epsilon \frac{A_o}{d_o} \qquad (1)$$

where d_o is the distance between CNT layers, q the charge between CNT layers, V the voltage between CNT layers, ϵ the permittivity of the material between the CNT layers, and A_o the overlapping area between two CNT layers. Under direct pressure, the PAN layer is compressed and the physical change in the distance d yields the capacitance variation.

In reality, the effects of temperature on the permittivity cause changes in capacitive output even in materials with a low temperature coefficient [7]. We estimate the effect of temperature on the permittivity $\beta = (\Delta\epsilon \mathbin{/} \epsilon) \mathbin{/} \Delta T$ of air gaps [8] and PAN [9] to be approx. –0.371% K^{-1} and 0.597% K^{-1} respectively, showing a higher likelihood of capacitance increasing with temperature. Thus, the main temperature dependence can be shown by

$$C = C_0(1 + \gamma \cdot \Delta T) \qquad (1)$$

where C_0 is the initial capacitance, γ the temperature coefficient of capacitance, and ΔT the change in temperature. Thus, when touching an object that has a different temperature from the sensor, the capacitance pickup can therefore be represented as

$$\frac{\Delta C_{P,T}}{C_0} = \frac{Ad_0 - dA_0}{A_0 d} + \gamma \cdot \Delta T \qquad (2)$$

Resistive temperature sensors

Neglecting the effects of pressure and physical deformations to the resistance, the embedded CNT layers sense the ambient temperature based on its reported TCR of –750 ppm/K [10], [11]. The internal CNT temperature reading can be used in conjunction with the pressure reading to provide thermal compensation without the need for additional sensors or circuitry. In a narrow range of temperatures (e.g. 25°C to 55°C), the main temperature dependence can be linearised by

$$R = R_0(1 + \alpha \cdot \Delta T) \qquad (4)$$

where R_0 is the initial resistance, α the temperature coefficient of resistance (TCR), and ΔT the change in temperature. Similarly, by substituting R for ρ the effects of temperature on the resistivity of the material can be found.

Materials and Fabrication

PAN nano-fibre was made by an electrospinning process using an applied voltage of 8 kV; and collected on a roller with speed of 500 rpm. The PAN (powder copolymer 99.5%AN/0.5%MA, Sigma Aldrich) was dissolved in dimethylformamide (N,N-dimethylformamide HCON(CH3)2, 99.0%, Sigma Aldrich) with a concentration of 10% (polymer/solvent).

Highly oriented Multi-Wall CNT (MW-CNT) films were pulled out from a CNT forest on a wafer. MW-CNTs with diameter of approx. 4 - 10 nm, length of 500 µm and high purity of carbon (> 99.9%) were synthetised by the chemical vapor deposition technique [12] . CNT films were stretched, layered on, and wrapped around the present sensor as the conductive medium. This was performed to achieve a soft, porous, and versatile surface electrode area. CNT is very thin and light and as such is a good material for using as a flexible electrode. However, CNT membranes are not suitable for direct physical contact such as touching or pressing. Electrospun PAN nano-fibre, on the other hand, is robust, low-cost, insulating, porous, lightweight, and thin material, which is ideal to protect and serve as dielectric layer.

Our presented sensor is fabricated *in situ* on a robot end effector. However, by modifying the PAN delivery process we believe it is possible to perform directly on human skin. As stated by Senthilkumar et al. [13], PAN is biocompatible and can be attached on the human body without any adverse impacts on human skin and the immune systems

Fabrication of our sensing device is performed *in situ* on an existing device (Baxter Robot) by electrospinning PAN onto the surface of the end effector to serve as the foundation (Figure 2 - Top). A layer of CNTs is laid over the PAN layer leaving a small gap on the non-sensing side for electrode application, further demonstration of placing CNT forest film and the control of its properties can be seen in [14], [15]. A layer of PAN is laid over the CNT layer as the dielectric. To avoid any shorting between CNT layers when connecting the electrodes, an insulator (Kapton polyimide tape) is applied over the areas where the electrodes will be attached before the second CNT layer is applied. A final PAN layer is introduced to encase and protect the sensor device. Parts of the PAN layer are carefully removed by a scalpel before adhering one electrode using silver epoxy to each CNT layer for pressure sensors or two on each layer for pressure and temperature sensing. The silver epoxy permeates through the porous fibres of the PAN and CNT to form robust electrical contacts.

The demonstrated sensor is fabricated as an example for robot applications. The Baxter Robots curved rubber end effector was utilised to demonstrate our present fabrication method and results. Figure 2 shows the close-up of fabricated sensor on the Baxter robot end effector and the SEM image of flexible and porous PAN and layered CNT fibres that assemble the sensor.

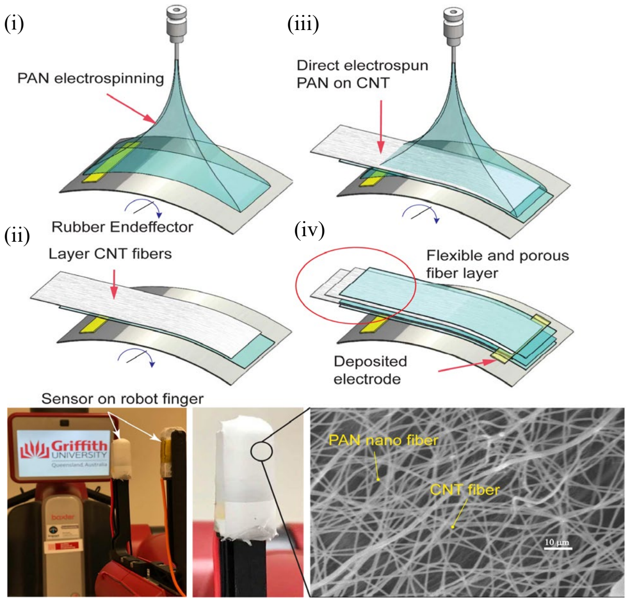

Figure 2. Formation of CNT-PAN sandwiched sensor: (Top) illustration of fabrication process, (i) electrospinning process to apply PAN to substrate, (ii) CNT is laid over the PAN layer of device, (iii-iv) repeat steps in i-ii. (Bottom) close-up of our in situ fabricated prototype sensor with Baxter robots end effector (Left); and SEM image of flexible and porous PAN and layered CNT fibres (Right).

CHARACTERISATION AND RESULTS

The resistive elements in our sensing device were firstly tested as heating elements. This was performed by supplying a constant current of 30 mA to one layer of CNTs. Figure 3 shows thermal images of the surface of our sensor matching the surface temperature of human skin, as can be seen in close proximity to a human fingertip. This would allow the fingertip to be tuned to a human-like temperature as necessary for human-robot interactions, providing a more human friendly interface subjectively compared to that of interactions with a cold device [16].

Demonstration of the e-skin is performed by monitoring our sensor, that was fabricated on the Baxter Robots finger, interacting with a temperature controlled graspable object. Dual Peltier modules (Adaptive Thermoelectric Generator Module GM250-127-14-16) attached to a solid aluminium block, with three embedded thermistors (STMicroelectronics LM335), was used as the gripped object (A schematic diagram of the experimental setup can be seen in Fig. 3).

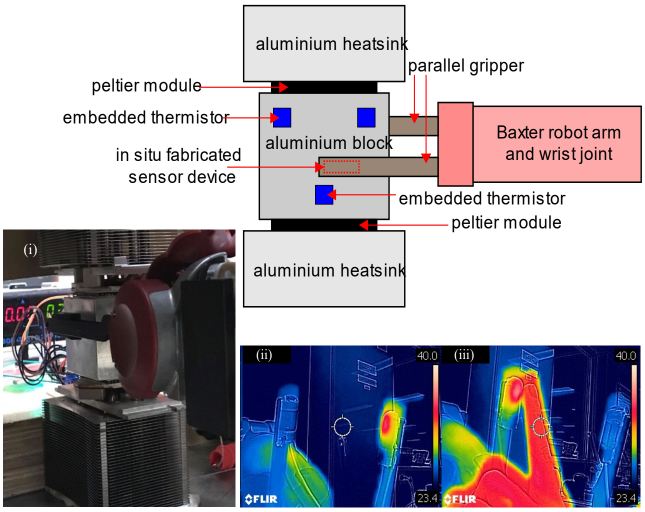

Figure 3. (Top) Schema of the experimental setup (Bottom) Robot finger shown used in heating mode: (i) heated robot finger, (ii) non-heated (left) and heated (right) robot fingers on Baxter's end effector, (iii) robot finger temperatures capable of matching that of human skin.

The sensor device was reassembled to the Baxter robot's parallel gripper and cyclic testing was performed using a specialised program in the ROS environment. The parallel grippers were controlled to repetitively grip and release using the maximum gripping parameters available (100% grip acceleration, moving force, holding force, etc.) in 5 second intervals. Measurements were performed using an LCR Meter (U1733C) and recorded automatically using the Keysight GUI Data Logger Software.

Figure 4 (a) shows the effect on resistance and capacitance with a constant gripping pressure under varied temperature. Alternatively, the opposite effect is demonstrated in Fig. 4 (b) where the sensor device is used as the heating element. A difference in the ambient temperature around the object and the direct surface temperature of the object causes the peaks as seen in Fig. 4(b)

Repetitive grasping at a constant temperature was performed to demonstrate the effect of pressure on the resistance. The grasped object maintains a differential of 0 °C between the object and room temperature. Grasping is easily recognisable by the sharp increase of the measured capacitance. The grasping capacitance signal is stable, and sensitivity does not change. Temperature resistance measurements in the sensor are stable, with minor noise of ± 0.1%.

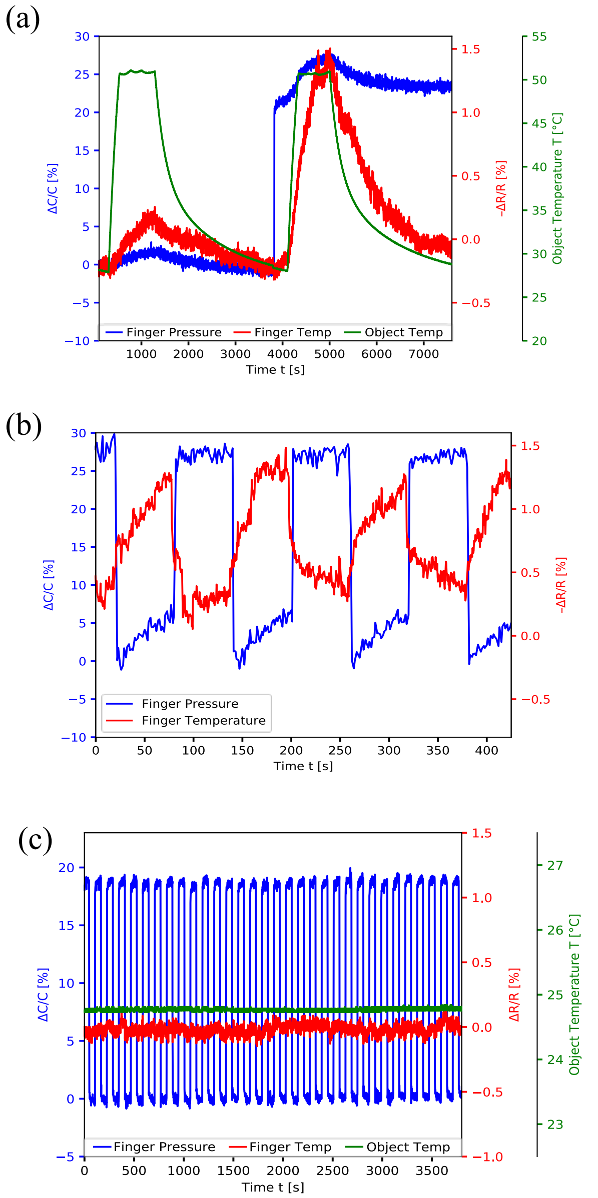

Figure 4. (a) Effects of varying temperature in proximity and under direct contact, (b) Gripping near-room temperature object while heating the integrated fingertip sensor on Baxter Robots parallel gripper, (c) Cycle testing: gripping a solid aluminium cube in a temperature-controlled environment. Varying temperature of gripped object, $\Delta T \approx 0.0$ °C. Ambient temperature, $T = 24.8$ °C. Estimated gripping force, $F \approx 11$ N. Estimated gripping pressure, $P \approx 48$ kPa. Object is kept at room (ambient) temperature.

CONCLUSIONS

We have demonstrated the design, fabrication, and application of a thin porous multimodal pressure and temperature sensitive e-skin device by fully integrating it into the curved surface of the Baxter Robot end effector utilising an *in situ* fabrication method. The device was capable of showing versatile functionality as a pressure sensor, temperature sensor, and heater. The robust, flexible, and stretchable CNT and PAN films were able to withstand long-term test with nearly no effects on the output signal. The fabrication process demonstrated in this work enables the development of multimodal sensing capabilities in e-skins for soft robotics, intelligent artificial and human-machine interfaces.

REFERENCES

[1] T. Someya and M. Amagai, “Toward a new generation of smart skins,” *Nat. Biotechnol.*, vol. 37, no. 4, pp. 382–388, Apr. 2019.

[2] Y. Gao, C. Lu, Y. Guohui, J. Sha, J. Tan, and F. Xuan, “Laser micro-structured pressure sensor with modulated sensitivity for electronic skins,” *Nanotechnology*, vol. 30, no. 32, 2019.

[3] W. Asghar *et al.*, “Piezocapacitive Flexible E-Skin Pressure Sensors Having Magnetically Grown Microstructures,” *Adv. Mater. Technol.*, vol. 5, no. 2, 2020.

[4] S. Chun, D. W. Kim, J. Kim, and C. Pang, “A transparent, glue-free, skin-attachable graphene pressure sensor with micropillars for skin-elasticity measurement,” *Nanotechnology*, vol. 30, no. 33, 2019.

[5] T. Yamaguchi, T. Kashiwagi, T. Arie, S. Akita, and K. Takei, “Human-Like Electronic Skin-Integrated Soft Robotic Hand,” *Adv. Intell. Syst.*, vol. 1, no. 2, p. 1900018, 2019.

[6] G. Franchi, A. Ten Pas, R. Platt, and S. Panzieri, “The Baxter Easyhand: A robot hand that costs $150 US in parts,” *IEEE Int. Conf. Intell. Robot. Syst.*, vol. 2015-December, pp. 2917–2922, 2015.

[7] J. Fastier-Wooller, T. Dinh, V. T. Dau, and D. V. Dao, “Soft ionic liquid multi-point touch sensor,” *RSC Adv.*, vol. 9, no. 19, pp. 10733–10738, 2019.

[8] A. W. Friend, “Charts of Dielectric Constant or Refractive Index of the Troposphere *,” *Bull. Am. Meteorol. Soc.*, vol. 29, no. 10, pp. 500–509, 1948.

[9] A. K. Gupta, R. P. Singhal, and V. K. Agarwal, “Effect of heat treatment on dielectric relaxation of polyacrylonitrile: Reversible thermally induced structural change,” *J. Appl. Polym. Sci.*, vol. 26, no. 11, pp. 3599–3608, 1981.

[10] T. Dinh *et al.*, “Polyacrylonitrile-carbon Nanotube-polyacrylonitrile: A Versatile Robust Platform for Flexible Multifunctional Electronic Devices in Medical Applications,” *Macromol. Mater. Eng.*, vol. 304, no. 6, 2019.

[11] V. T. Dau, C. D. Tran, T. T. Bui, V. D. X. Nguyen, and T. X. Dinh, “Piezo-resistive and thermo-resistance effects of highly-aligned CNT based macrostructures,” *RSC Adv.*, vol. 6, no. 108, 2016.

[12] C. D. Tran, S. Lucas, D. G. Phillips, L. K. Randeniya, R. H. Baughman, and T. Tran-Cong, “Manufacturing polymer/carbon nanotube composite using a novel direct process,” *Nanotechnology*, vol. 22, no. 14, p. 145302, 2011.

[13] S. Senthilkumar, S. Rajesh, A. Jayalakshmi, and D. Mohan, “Biocompatibility studies of polyacrylonitrile membranes modified with carboxylated polyetherimide,” *Mater. Sci. Eng. C*, vol. 33, no. 7, pp. 3615–3626, 2013.

[14] C. D. Tran, K. Le-Cao, T. T. Bui, and V. T. Dau, “Dielectrophoresis can control the density of CNT membranes as confirmed by experiment and dissipative particle simulation,” *Carbon N. Y.*, vol. 155, pp. 279–286, 2019.

[15] V. T. Dau, D. V. Dao, T. Yamada, B. T. Tung, K. Hata, and S. Sugiyama, “Integration of SWNT film into MEMS for a micro-thermoelectric device,” *Smart Mater. Struct.*, vol. 19, no. 7, 2010.

[16] E. Park and J. Lee, “I am a warm robot: The effects of temperature in physical human-robot interaction,” *Robotica*, vol. 32, no. 1, pp. 133–142, 2014.

CONTACT

*Jarred W. Fastier-Wooller (jarred.fastier-wooller@griffithuni.edu.au)